Investigating Climate-Driven Slope Failures Using Centrifuge Modelling and Pore Water Pressure Analysis

Muna A. Alfergani, Elisabeth T. Bowman and Tawfeg Elmrom
School of Mechanical, Aerospace and Civil Engineering
University of Sheffield, Sheffield, The UK
maalfergani@gmail.com, e.bowman@sheffield.ac.uk, telmrom@gmail.com

ABSTRACT: This study provides new insights into rainfall- and flood-induced slope failure through high-fidelity physical centrifuge modelling combined with pore water pressure (PWP) analysis. A series of model tests was conducted under controlled seasonal climate simulations representative of UK conditions, incorporating repeated "winter-type" rainfall phases, summer drying periods, controlled flooding events, and gradual drawdown processes. The experimental setup featured dense arrays of high-resolution PWP sensors to capture transient hydromechanical responses across both stable and failed slope models. To reconstruct the internal pore pressure field between discrete points, the GRIDFIT method (D'Errico, 2006) was implemented in MATLAB to generate continuous PWP contours. Unlike conventional interpolation techniques, GRIDFIT solves the standardised least squares problem to produce smooth, noise-tolerant surface models that preserve both spatial fidelity and the physical behaviour of geotechnical data. This enabled the precise visualisation of subsurface pressure concentrations, particularly along developing failure surfaces. The results clearly demonstrate the link between pore pressure and slope instability at failure, and they also highlight the value of combining dense instrumentation with advanced modelling tools. This work establishes a replicable framework for quantifying subsurface hydraulic conditions in physical models and offers a benchmark for assessing climate-driven slope failures with high spatial and temporal resolution.

1 INTRODUCTION

Climate change is intensifying rainfall events and flood hazards, which in turn threaten the stability of engineered slopes and embankments, in particular those that are deigned as flood embankments or levees (Legg, 2021, Westra et al., 2013, Trenberth, 2011). In the UK, rainfall-induced failures represent a major geotechnical challenge for transport and flood defence infrastructure (Dijkstra and Dixon, 2010, Smethurst et al., 2012). Conventional numerical analyses have limitations in capturing complex transient pore water pressure responses under climate-driven conditions (Rahardjo et al., 2007, Bogaard and Greco, 2016, Iverson, 2000). Physical modelling, particularly centrifuge modelling, provides a means of replicating realistic stress and hydraulic conditions at model scale (Schofield, 1980). Previous studies (Take et al., 2004) have shown the influence of rainfall infiltration and drawdown on slope stability, but there remains a need for higher-resolution experimental data and improved methods of visualising subsurface pore pressures. This study contributes by combining (i) dense PWP instrumentation, (ii) climate scenario simulations, and (iii) GRIDFIT-based reconstruction of pore pressure fields.

2 EXPERIMENTAL METHODOLOGY

A series of centrifuge model tests was conducted to investigate the pore water pressure (PWP) response and failure mechanisms of a compacted slope subjected to rainfall, flooding, and drawdown. The experimental program was performed using the 2m raidus geotechnical centrifuge at the University of Sheffield, which allows realistic stress conditions to be reproduced on a reduced scale. Scaling laws following (Schofield, 1980) were applied to ensure that the model stress state, seepage behaviour, and timescale were consistent with prototype conditions.

2.1 Soil and Model Preparation

The slope was constructed by compaction at optimum moisture content using a mixture of 65% sand and 35% kaolin, chosen to reproduce the low permeability and plasticity typical of UK clay embankments.

Laboratory tests determined key parameters, including permeability (falling head) $k = 9.8 \times 10^{-10}$ m/s, shear strength (consolidated drained triaxial) $\phi'_{crit} = 26.6°$, and compressibility (oedometer) $m_v = 0.0002$ kN/m^2. The slope geometry was built at 1V:1.5H (~33°).

2.2 Instrumentation

An array of 11 PWP sensors was embedded at multiple depths across the slope as shown in Figure 1. This dense configuration set out in columnar arrays allowed transient pore pressures to be captured and later interpolated into continuous fields. The column-style layout also facilitated comparison with numerical modelling (not covered in this paper).

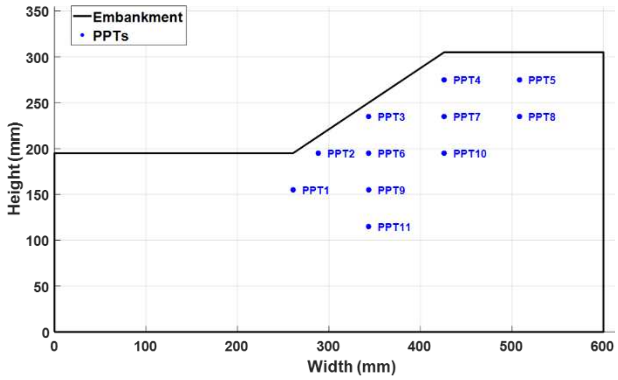

Figure 1. Slope dimension and PPTs locations.

2.3 Climate Scenario and Hydraulic Loading

A climate sequence simulated typical UK seasonal conditions with each winter phase consisting of approximately seven months at prototype scale with increasing winter rainfall severity across the experiment. Each summer phase was modelled as a five month dry period with no rainfall to simulate low-moisture conditions. After a fully dry period in which the pore pressures equilibrated for three months after centrifuge spin up, Winter 1 consisted of repeated cycles of one week of rainfall followed by one week of no rainfall. After Summer 1, Winter 2 intensified the wetting pattern to two weeks of rainfall and one week of drying, while after Summer 2, Winter 3 adopted three weeks of rainfall followed by one week of drying. Subsequently, additional hydraulic loading was introduced through controlled flooding and drawdown, during which water levels were raised and lowered over ten equivalent days at prototype-consistent rates. This combined climate–hydraulic sequence generated realistic transient pore-water pressure variations within the slope.

3 DATA PROCESSING

The pore water pressure (PWP) readings obtained from the transducers were first baseline-corrected using hydrostatic offsets to ensure that subsequent variations reflected true transient responses. To visualise the spatial distribution of pore pressures within the slope, the GRIDFIT algorithm (D'Errico, 2006) was implemented in MATLAB. GRIDFIT solves a regularised least-squares surface-fitting problem to generate smooth and continuous surfaces from discrete sensor readings. This approach is particularly advantageous for geotechnical data because it:

- Minimises the influence of sensor noise
- Preserves realistic hydraulic gradients

In this study, GRIDFIT was used to interpolate PWP measurements across the slope cross-section for selected time intervals. The resulting contour plots provided a continuous visualisation of the transient pore pressure field, enabling the identification of localised zones of elevated pressure that were aligned with the observed failure surface.

4 RESULTS AND DISCUSSION

4.1 Pore Pressures under Rainfall

The rainfall phases in the test produced a gradual rise in pore water pressures within the slope. Sensors located near the mid-slope and toe recorded the most significant increases, indicating limited drainage and partial pressure accumulation over successive cycles. Each rainfall week was followed by a week without rainfall, with pore pressures indicating progressive retention of water within the lower layers.

Figure 2 (End of Summer 1) represents the PWP field after the summer drying phase.

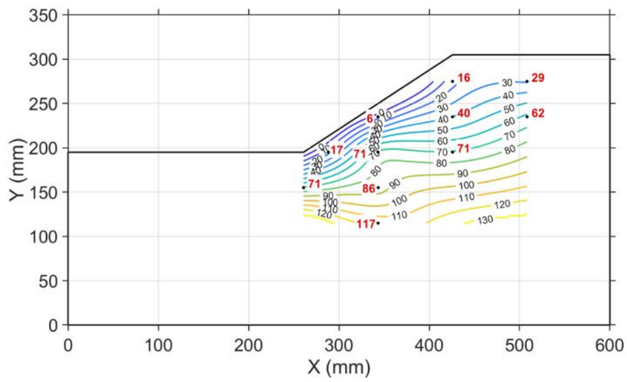

Figure 2. Pore pressure at the end of Summer 1.

Although no rainfall occurs during the summer, the figure shows that a significant portion of the pore pressure generated during the preceding winter (not shown) remained within the slope. The PWP field at the end of Winter 2 (Figure 3) shows only a minor change relative to the distribution observed at the end of Summer 1. However, a localised increase in pore water pressure at PPT2 is evident, reflecting continued wetting during the second winter and incomplete dissipation in the mid-slope region. Overall, the contour pattern remains similar, indicating limited drainage and no major change in the hydraulic regime during Winter 2.

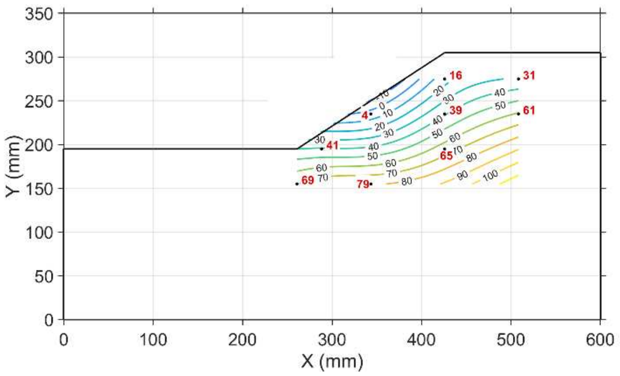

Figure 3. Pore pressure at the end of Winter 2.

The following section examines the pore pressure changes that occurred during a shallow slope failure which took place during Winter 2. This was just detectable in the GeoPIV (Geotechnical Particle Image Velocimetry) analysis (White et al., 2003) taken at the sidewall of the experiment but was not discernible to the naked eye.

4.2 Winter 2 Failure Mechanism Based on PWP Measurements.

The Winter 2 failure coincided with a sudden pore pressure spike followed by an abrupt reduction, as recorded by PPT3. This spike coincided with the small shallow failure in the slope discussed above. This pattern reflects a rapid transition from compression to dilation within a zone of failure. Initial compression generated excess pore pressure as the soil structure contracted under shear, followed by dilation once the slip surface developed, leading to a sharp pressure drop as pore water expanded into newly formed voids.

As shown in Figure 4, the onset of failure during the second winter occurred between approximately 12360s and 12383s, as indicated by the ΔP time histories. This interval corresponds to 2382–2405s after the start of Winter 2 at model scale, which, under 70g centrifuge scaling, equates to approximately 135.1–136.4 days in prototype time or around 4.5 months. The failure duration was over 31.3 h, or ~1.3 days at prototype. The PWP evolution during this short interval reveals a clear transition from hydraulic loading controlled behaviour to mechanically induced pore pressure changes associated with shear deformation.

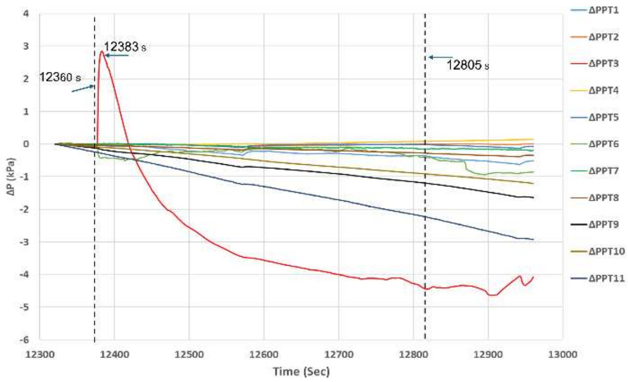

Figure 4. ΔP Response During Winter 2 Failure Event.

At 12360s, the slope had already undergone several months (prototype time) of winter rainfall, which progressively elevated pore pressures across the mid-slope and toe. The corresponding PWP contour (Figure 5) shows a gentle pressure gradient extended upward towards the crest. This state represents an accumulated hydraulic load from repeated winter rainfall cycles. Although no failure had yet occurred, the slope was in a weakened condition with reduced effective stress.

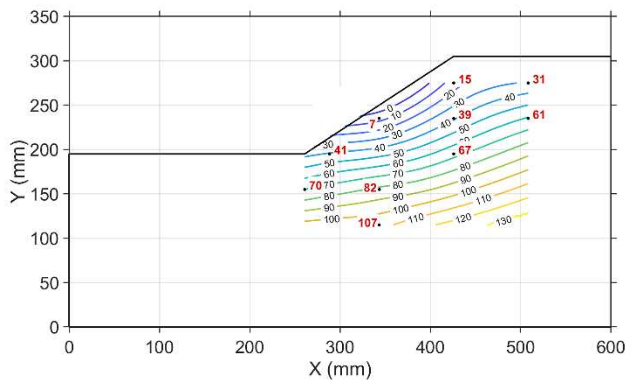

Figure 5. Pore Water Pressure Contours Before Winter 2 Failure (12360s).

Between 12360s and 12383s, the pore pressure readings show two successive changes:

1. A sudden rise in ΔP (especially at PPT3).
2. An abrupt drop immediately afterward, typical of dilation following peak shear.

The contour at 12383s (Figure 6) captures this moment. This behaviour is characteristic of contractive shearing within a developing slip zone. As the soil contracts, water attempts to be expelled, causing a transient positive pore pressure spike. The sudden drop immediately after reflects dilation as the shear band fully forms.

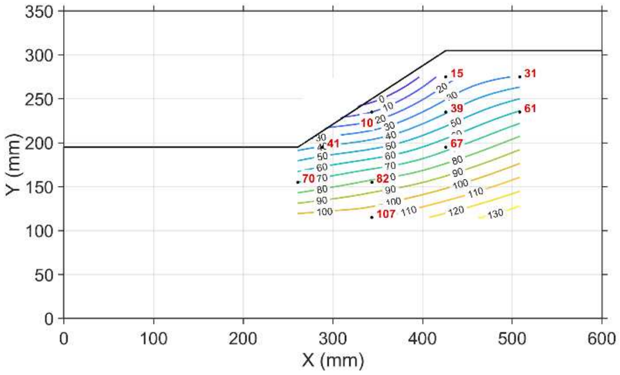

Figure 6. Pore Water Pressure Contours at Winter 2 Failure (12383 s).

By 12805s after the onset of failure, the PWP contours (Figure 7) show a clear reduction in pore pressures across the mid-slope and lower-slope regions compared with the pre- and at-failure states. The high-pressure concentrations that were previously localised around the developing shear surface have largely dissipated.

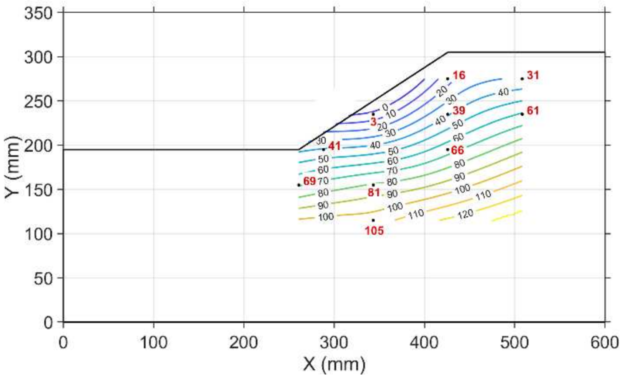

Figure 7. Pore Water Pressure Contours After Winter 2 Failure (12805s).

4.3 PWP Response during Flooding

Summer 2 and Winter 3 (not shown) reveal similar pore pressure profiles as the preceding Summer 1 and Winter 2. Subsequent to these seasonal variations, several controlled flooding and drawdown scenarios were investigated.

Controlled flooding caused an immediate rise in pore pressures across the lower part of the slope. As shown in Figure 8, the highest pressures developed at the toe, where values reached approximately 110-123 kPa. These values reflect the hydraulic loading imposed by the rising external water level. The hydrostatic pressure calculated from the floodwater level was used to determine the appropriate sensor offset for the pore pressure data in the preceding data, so that the recorded measurements aligned with the expected total head during flooding. Mid-slope sensors recorded increases in the range of 70–90 kPa, while sensors nearer the crest showed more moderate values.

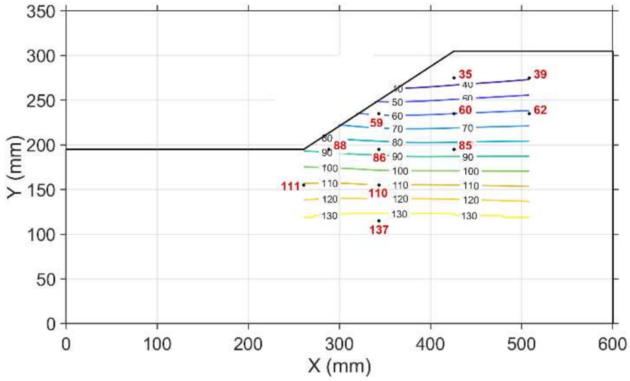

Figure 8. Pore pressure during first flood.

4.4 PWP during Drawdown

During gradual drawdown over a prototype period of 10 days, pore pressures within the slope decreased, but dissipation lagged the falling external water level. As shown in Figure 9, this delayed response created a transient outward seepage condition, generating localised positive pore pressures near the lower slope face. Such conditions are known to reduce effective stress and compromise stability. The persistence of elevated pore pressures in this test demonstrates the critical influence of drawdown rates on slope safety.

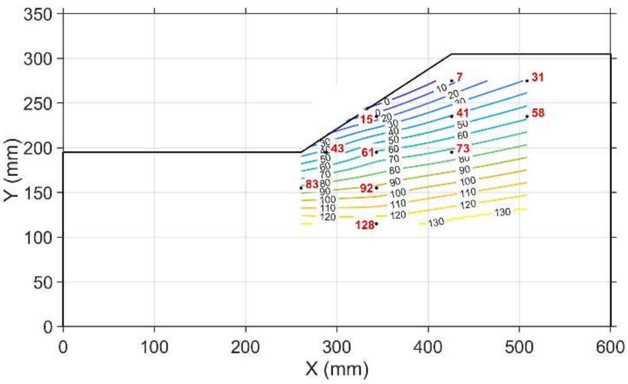

Figure 9. Pore pressure at the end of first drawdown (when the water reaches the toe at Y=195mm).

4.5 Discussion

The main contributions and innovations to this study:

(1) If a suitably high number of PPTs are used, it may be possible to intercept the failure surface explicitly, which was the case here. The response

of the specific PPT in question (contraction and dilation in the localised shear zone) indicated the nature of the failure even when there was little observable shear deformation.

(2) GRIDFIT is a useful tool to develop PPT (and potentially other sensor signal) contours in physical modelling as it is agnostic to the specific nature of the signals themselves.

(3) Centrifuge modelling can used for both prefailure and postfailure response of slopes that may be continuously subjected to cyclic environmental loading.

The test results confirmed the cumulative effect of rainfall, flooding, and drawdown on pore pressure generation. Rainfall produced gradual increases in pore pressure while localised pore pressure changes were found in PPTs close to the failure surface during rainfall application. Flooding induced a rapid pore pressure rise at the toe and relatively rapid drawdown (over 10 days) led to delayed PWP dissipation, maintaining positive pore pressures and triggering further instability.

These results emphasise that even moderate rainfall and flood / drawdown sequences can create critical pore pressure conditions leading to failure and ongoing deformation. The GRIDFIT reconstructions effectively captured the internal redistribution of pore pressure and revealed the spatial correlation between PWP peaks and failure zones.

A limitation of this study were that extreme weather conditions were not modelled in the box as it was not completely sealed (so "Summer" was not especially hot), although "typical" to UK conditions were covered. Also, the study only looked at very low plasticity sandy-clay behaviour and very low suction values were not developed at the surface (due to the Summer modelling period not being especially hot).

5 CONCLUSIONS

This study investigated the pore water pressure (PWP) behaviour of a reconstituted sand–kaolin slope subjected to rainfall, flooding, and drawdown under centrifuge conditions. The test provided comprehensive understanding of the transient hydraulic mechanisms that control slope stability under climate-driven loading. The use of GRIDFIT enabled noise-tolerant, smooth contour mapping that preserved realistic gradients, offering a clearer visualisation of transient subsurface conditions than conventional interpolation methods. The findings highlight the combined impact of rainfall infiltration, flooding, and moderate drawdown on pore pressure evolution. Even gradual hydrological changes can lead to instability when dissipation is restricted. The experimental approach provides a replicable framework for assessing climate-driven slope failure mechanisms.

ACKNOWLEDGEMENTS

The authors would like to thank the technical staff, particularly Mr Mark Foster, at the University of Sheffield for their assistance during the centrifuge testing. The authors also acknowledge the contribution of Dr Tiago Gaspar (Imperial College London), who provided helpful advice.

REFERENCES

Bogaard, T. A. & Greco, R. 2016. Landslide hydrology: from hydrology to pore pressure. *Wiley Interdisciplinary Reviews: Water,* 3**,** 439-459. doi.org/10.1002/wat2.1126

D'Errico, J. 2006. Surface fitting using gridfit (http://www. mathworks. com/matlabcentral/fileexchange/8998), MATLAB® Central File Exchange. *Retrieved May,* 18**,** 2006.

Dijkstra, T. & Dixon, N. Climate change and slope stability in the UK: challenges and approaches. 2010. Geological Society of London. doi.org/10.1144/1470-9236/09-036

Iverson, R. M. 2000. Landslide triggering by rain infiltration. *Water Resources Research,* 36**,** 1897-1910. doi.org/10.1029/2000WR900090

Legg, S. 2021. IPCC, 2021: Climate change 2021-the physical science basis. *Interaction,* 49**,** 44-45.

Rahardjo, H., Ong, T., Rezaur, R. & Leong, E. C. 2007. Factors controlling instability of homogeneous soil slopes under rainfall. *Journal of Geotechnical and Geoenvironmental Engineering,* 133**,** 1532-1543.

Schofield, A. N. 1980. Cambridge geotechnical centrifuge operations. *Géotechnique,* 30**,** 227-268. doi.org/10.1680/geot.1980.30.3.227.

Smethurst, J., Clarke, D. & Powrie, W. 2012. Factors controlling the seasonal variation in soil water content and pore water pressures within a lightly vegetated clay slope. *Géotechnique,* 62**,** 429-446, doi.org/10.1680/geot.10.P.097.

Take, W., Bolton, M., Wong, P. & Yeung, F. 2004. Evaluation of landslide triggering mechanisms in model fill slopes. *Landslides,* 1**,** 173-184. doi.org/10.1007/s10346-004-0025-1

Trenberth, K. E. 2011. Changes in precipitation with climate change. *Climate Research,* 47**,** 123-138.

Westra, S., Alexander, L. V. & Zwiers, F. W. 2013. Global increasing trends in annual maximum daily precipitation. *Journal of Climate,* 26**,** 3904-3918.

White, D., Take, W. & Bolton, M. 2003. Soil deformation measurement using particle image velocimetry (PIV) and photogrammetry. *Géotechnique,* 53**,** 619-631, doi.org/10.1680/geot.2003.53.7.619.